An RNA-binding tropomyosin recruits kinesin-1 dynamically to *oskar* mRNPs

Imre Gáspár*, Vasily Sysoev, Artem Komissarov and Anne Ephrussi*

Developmental Biology Unit, European Molecular Biology Laboratory, Meyerhofstrasse 1, Heidelberg,D-69117, Germany

*Corresponding authors: Anne Ephrussi, e-mail: ephrussi@embl.de, tel: +49-6221-387-8429

Imre Gáspár: e-mail: gaspar@embl.de, tel: +49-6221-387-8845

Abstract

Localization and local translation of *oskar* mRNA at the posterior pole of the *Drosophila* oocyte directs abdominal patterning and germline formation in the embryo. The process requires precise recruitment and regulation of motor proteins to form transport-competent mRNPs. Using high- and super-resolution imaging, we determine the steps in motor recruitment to *oskar* mRNPs. We show that the posterior-targeting kinesin-1 is recruited upon nuclear export of *oskar* mRNPs, prior to their dynein-dependent transport from the nurse cells into the oocyte. We demonstrate that *Dm*Tropomyosin1-I/C is an atypical RNA-binding, nucleocytoplasmic shuttling Tropomyosin1 isoform that binds the *oskar* 3'UTR through recognition of a supramolecular RNA motif created upon dimerization of *oskar* molecules. Our data show that, in the oocyte, kinesin-1 is recruited by *Dm*Tropomyosin1-I/C to a dynamically changing, small subset of *oskar* mRNPs and is activated by the functionalized spliced *oskar* RNA localization element, revealing an ergonomic, coordinated mechanism of cargo transport.

Highlights:

- *Drosophila* Tropomyosin1-I/C is an RNA-binding, nucleocytoplasmic shuttling protein
- DmTm1-I/C dynamically recruits Khc to *oskar* mRNPs
- DmTm1-I/C preferentially binds an RNA motif formed upon dimerization of *oskar* 3' UTRs
- The exon junction complex/spliced *oskar* localization element complex is endowed with kinesin activating function

Introduction

Within cells, diverse macromolecules, complexes, and organelles are distributed by a small set of cytoskeleton-associated motor proteins. Appropriate delivery is achieved by cargo-associated guidance cues that are responsible for recruiting the appropriate mechanoenzyme[1]. Such actively transported cargoes include mRNAs, whose asymmetric localization and local translation within cells have been shown to be essential for various cellular functions, such as migration, maintenance of polarity and cell fate specification[2]. In the case of messenger ribonucleoprotein (mRNP) particles, the guidance cues are the mRNA localization elements (LE) that suffice to drive localization of any RNA molecule that contains them[3]. A few LEs, their RNA binding proteins (RBP) and the factors that link them to the mechanoenzyme have been well characterized[4-7]. In these cases, the entire localization process is driven by a single type of motor. Other mRNAs, such as *Xenopus laevis Vg1*[8] or *Drosophila melanogaster oskar (oskar)*[9-11] rely on the coordinated action of multiple motor proteins - cytoplasmic dynein and kinesin-1 and -2 family members - for their localization within developing oocytes.

oskar mRNA encodes the posterior determinant Oskar protein, which induces abdomen and germline formation in a dosage-dependent manner in the fly embryo[12]. *oskar* mRNA is transcribed in the nurse cells of the germline syncytium and transported into the oocyte, similarly to e.g. *bicoid* and *gurken* mRNAs[13, 14]. This first step of *oskar* transport is guided by a well described LE, the oocyte entry signal found in the 3'UTR of the mRNA[10], which is thought to recruit the Egl-BicD-dynein transport machinery[9, 10]. In the oocyte, *oskar* mRNA localization to the posterior pole is mediated by kinesin-1[11, 15, 16]. This second step of *oskar* transport requires splicing[17], which assembles the spliced localization element (SOLE) and deposits the exon junction complex (EJC) on the mRNA, to form a functional EJC/SOLE posterior targeting unit[18]. The EJC/SOLE was shown to be crucial for maintaining efficient kinesin-1 dependent transport of *oskar* mRNPs within the oocyte[11, 18], which is essential for proper localization of the mRNA to the posterior pole.

In a forward genetic screen, a group of *DmTm1* (formerly *DmTmII*) mutants (*Tm1*^{gs}) was identified in which *oskar* mRNA accumulation at the posterior pole of the oocyte fails[11, 19] (Fig. 1a,b). Although the small amount of Oskar protein produced at the posterior pole is sufficient for embryo progeny of *Tm1*^{gs} homozygous females to form an abdomen and develop into adult flies, it is insufficient to induce primordial germ cell formation. Consequently, the *Tm1*^{gs} progeny are sterile, resulting in a so-called 'grandchildless' phenotype[19]. It was subsequently demonstrated that the microtubule mediated intra-ooplasmic motility of *oskar* mRNPs is affected in *Tm1*^{gs} mutants[11] (Supplementary Table 1), similar to what has been observed when kinesin-1 is absent[11]. Although there is biochemical evidence that kinesin-1 associates with *oskar* mRNPs[20], what mediates its association with the mRNA and where in the egg-chamber this occurs is not known.

Here, we demonstrate that DmTm1-I/C, a product of the *DmTm1* locus, is an RNA binding tropomyosin that recruits kinesin heavy chain (Khc) to *oskar* mRNA molecules as soon as they are exported from the nurse cell nuclei. Within the ooplasm, Khc recruitment is transient and dynamic and this dynamicity depends on the presence of DmTm1-I/C. Our data indicate that the EJC/SOLE triggers kinesin-1 activity within the oocyte during mid-oogenesis to ensure proper localization of *oskar* mRNA.

Results

Tm1-I maintains kinesin-1 on *oskar* mRNA

To obtain mechanistic information regarding the motility defect in *Tm1*^{gs} oocytes, we developed an *ex vivo* assay that allows co-visualization of MS2-tagged *oskar* mRNPs and polarity-marked microtubules (MTs) in ooplasm and determination of the directionality of *oskar* mRNP runs (Fig. 1c, Supplementary Fig. 1a and Supplementary Movie 1), thus giving insight into the identity of the motor(s) affected by the *Tm1*^{gs} mutations. Using this assay, we found that in wild-type ooplasm plus end-directed runs of *oskMS2* RNPs dominated about two to one over minus end-directed runs (Fig. 1d). Plus-end dominance was lost both in ooplasm lacking Khc and in extracts prepared from *Tm1*^{gs} mutant oocytes (Fig. 1d). This indicates that plus end-directed, Khc-mediated motility is selectively compromised in the *Tm1*^{gs} mutants. The remaining plus end directed runs might be due to residual kinesin-1 activity, to other plus end-directed kinesins, or to cytoplasmic dynein, which has been shown to mediate the bidirectional random walks of mRNPs along MTs[21]. To test if the loss of Khc activity might be the cause of *oskar* mislocalization in *Tm1*^{gs} oocytes, we tethered a minimal Khc motor, Khc$_{401}$[22, 23], to the MS2-tagged *oskar* mRNPs. Co-expression of Khc$_{401}$ –MCP and *oskMS2* restored the plus end dominance of *oskar* mRNP runs (Fig. 1d), as well as localization of *oskar* mRNA (Fig. 1e,f), confirming that loss of kinesin-1 activity might cause *oskar* mislocalization in *Tm1*^{gs} mutants.

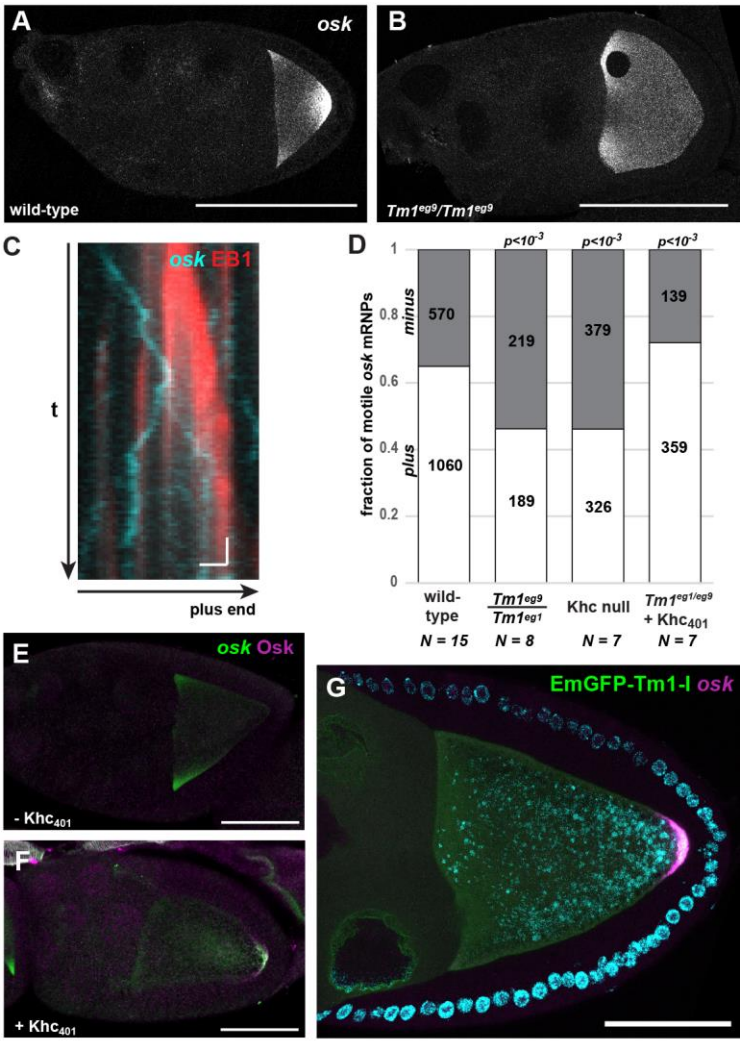

Figure 1: Localization of *oskar* mRNA in wild-type control (**a**) and in $Tm1^{eg9}/Tm1^{eg9}$ (**b**) egg-chambers. (**c**) Kymograph of *oskMS2*-GFP mRNPs (cyan) travelling along polarity marked MTs (red, EB1 protein) in an *ex vivo* ooplasmic preparation. Scale bars represent 1 s and 1 µm, respectively. (**d**) Distribution of *oskMS2*-GFP mRNP runs towards plus (white) and minus ends (gray). Numbers within the bars indicate number of runs. P value of Chi^2 test against wild-type is indicated above each bar. *oskar* mRNA (green) and Oskar protein (magenta) distribution in $Tm1^{eg1}/Tm1^{eg9}$ egg-chambers expressing *oskarMS2(6x)* (**e**) or *oskarMS2(6x)* and Khc_{401}-MCP (**f**). (**g**) *oskar* mRNA (magenta) distribution in $Tm1^{eg1}/Tm1^{eg9}$ egg-chambers rescued with EmGFP-Tm1-I (green). Scale bars represent 50 µm. See also Supplementary Figs 1 and 4 and Movie 1.

The *DmTm1* locus encodes 17 different transcripts and 16 different polypeptides (Supplementary Fig. S2a). By performing semi-quantitative RT-PCR analysis, we found that the transcripts of Tm1-C, I and H are selectively missing or their amount is greatly reduced in $Tm1^{eg1}$ and $Tm1^{eg9}$ homozygous ovaries, respectively (Supplementary Fig. S2b,c). An EmGFP-Tm1-I transgene expressed in the female germline rescued *oskar* mislocalization

(Fig. 1g) and the consequent grandchildless phenotype of *Tm1*^{gs} mutants (all female progeny – 20+ - contained at least one ovary with developing egg-chambers), indicating that function of the Tm1-I/C isoform is essential for *oskar* mRNA localization.

To determine whether the reduction in Khc-dependent *oskar* mRNP motility in *Tm1*^{gs} oocytes is due to an inefficient activation of the motor or rather to insufficient recruitment of kinesin-1, we analysed the composition of *oskar* mRNPs *ex vivo*. Our object-based colocalization analysis of single snapshot images corrected for random colocalization (Supplementary Fig. 1e-h) revealed that both Khc-EGFP (Fig. 2a and Supplementary Movie 2) and EmGFP-Tm1-I (Fig. 2b and Supplementary Movie 3) are recruited to a significant fraction of *oskMS2*-mCherry mRNPs, indicating that both proteins are components of *oskar* transport particles (Fig. 2c). In *Tm1*^{gs} mutant extracts, we observed a significant, 2-4 fold reduction in the fraction of Khc-positive *oskar* mRNPs compared to the wild-type controls (Fig. 2d). This indicates that the observed motility and localization defects in *Tm1*^{gs} are due to insufficient kinesin-1 recruitment to *oskar* mRNPs. When we performed immunoprecipitations from ovarian lysates, Khc and Staufen, but no other tested *oskar* RNP components (Bruno, Y14, BicD or dynein), co-immunoprecipitated specifically with the EmGFP-Tm1-I bait (Fig. 2e). Although such an *en mass* co-immunoprecipitation analysis lacks spatiotemporal resolution, it suggests that Tm1-I/C, kinesin-1 and Staufen form stable complexes with each other that are maintained by – not necessarily direct - protein-protein interactions.

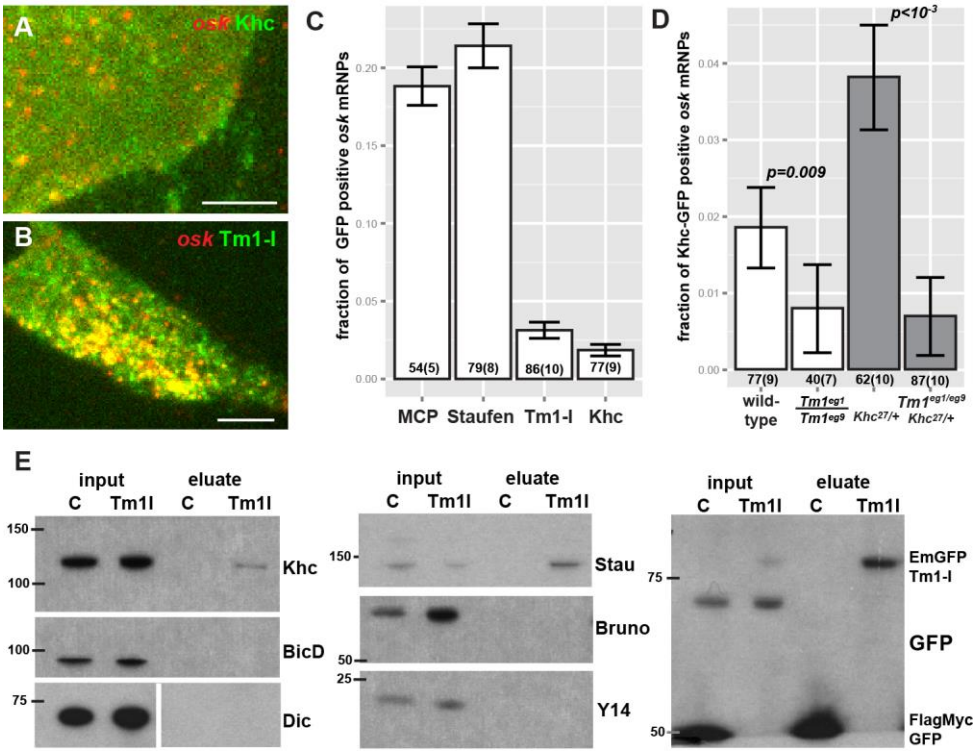

Figure 2: Colocalization of *oskMS2*-mCherry with Khc-EGFP (**a**) or with EmGFP-Tm1-I (**b**) in *ex vivo* ooplasmic preparations. (**c**) Fraction of *oskMS2*-mCherry mRNPs located non-randomly within a 200 nm distance of one of the indicated GFP tagged protein particles in *ex vivo* ooplasmic preparations. All values are significantly different from zero ($p<10^{-3}$, one sample t-test). (**d**) Fraction of *oskMS2*-mCherry mRNPs co-localizing (max. 200 nm) non-randomly with Khc-EGFP particles in wild-type and in $Tm1^{eg1}/Tm1^{eg9}$ ooplasmic squashes in presence of two (white) or one (gray) copy of endogenous Khc. P values of two sample t-tests are indicated above the relevant bar pairs (**c, d**). Numbers indicate the number of particle clusters (number of preparations) analysed. Error bars represent 95% confidence intervals. . (**e**) Western blots of *oskar* mRNP components (Staufen, Bruno and Y14) and motor associated proteins (Khc, BicD, Dic) co-immunoprecipitated with EmGFP-Tm1-I from ovarian lysates. Protein marker bands and their molecular weight in kDa are indicated. See also Supplementary Fig. 1 and Movies 2 and 3.

Kinesin-1 associates dynamically with *oskar* RNPs

The amount of colocalization of EmGFP-Tm1-I or Khc-EGFP with *oskar* mRNA we observed was substantially less than of GFP-Staufen, a *bona fide* partner of *oskar* mRNA[11] (Fig. 2c). We reasoned that this might be due to the presence of endogenous unlabelled protein molecules, particularly affecting Khc-EGFP colocalization measurements (Fig. 2d and Supplementary Fig. 2c,f). To improve the labelling ratio, we fluorescently tagged Khc and Tm1 at their endogenous loci. Although these alleles allowed us to label virtually all Khc and Tm1-I/C molecules (Supplementary Fig. 2c,g), we did not detect a substantial increase in Khc-

associated *oskar* RNPs due to the greater crowding of the labelled molecules and the consequent elevated frequency of random events (Supplementary Fig. 3a,b). To circumvent this problem, we analysed time series (Fig. 3a,b and Supplementary Fig. 3c), since the likelihood of random co-localization (~13% at 250 nm distance in case of a single tagged Khc^{mKate2} allele in a single snapshot image, Supplementary Fig. 3b) decreases progressively when co-localization is observed in multiple frames along an *oskar* RNP trajectory (Supplementary Fig. 3c).

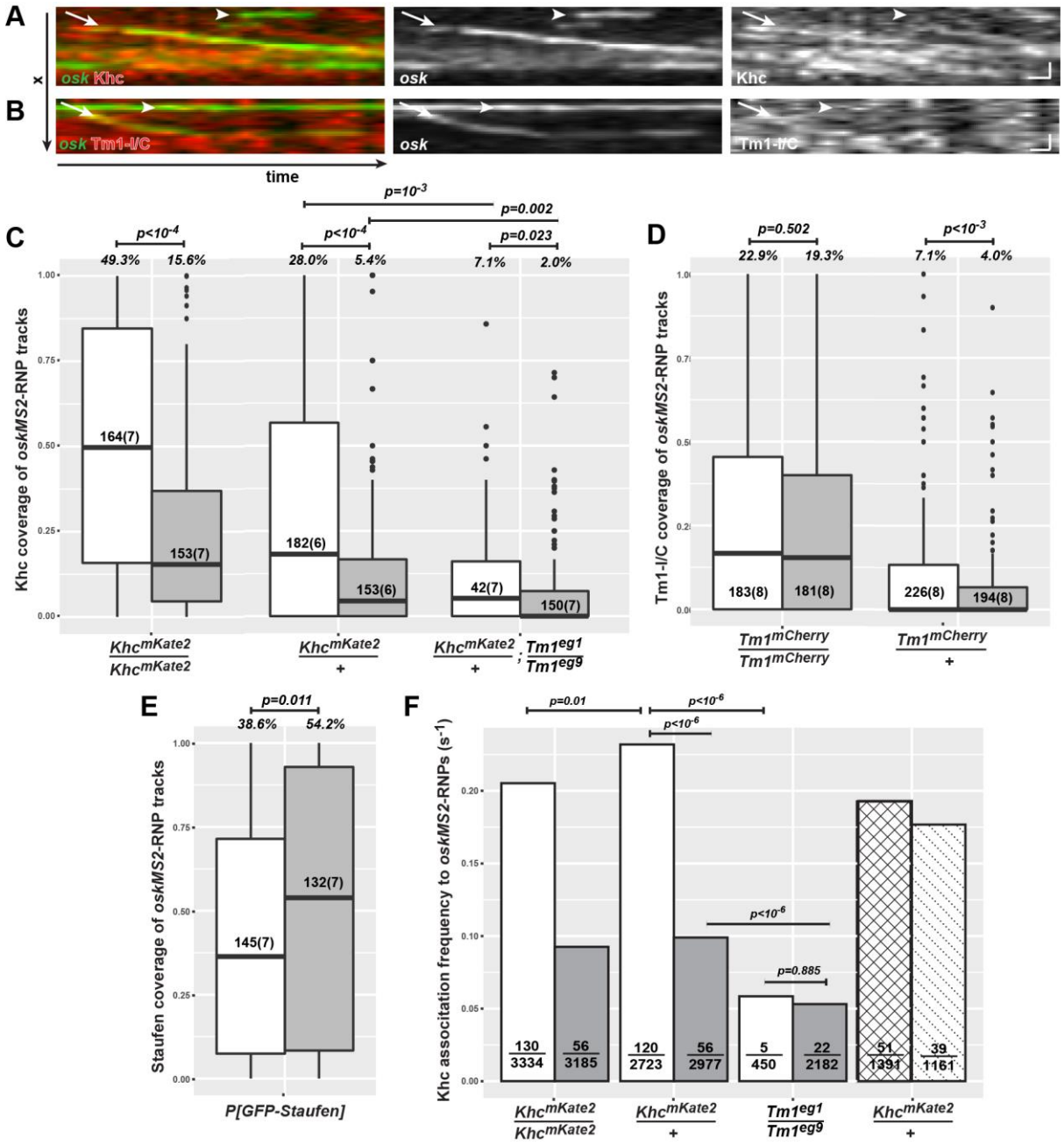

Figure 3: Kymographs of *oskMS2*-GFP mRNPs (green) associated with Khc-mKate2 (**a**, red) and mCherry-Tm1-I/C (**b**, red) *ex vivo*. Arrows indicate motile RNPs in stable complex with Khc (**a**) or Tm1-I/C (**b**), the arrowheads point to non-motile *oskMS2*-RNPs showing no obvious accumulation of the tagged protein. Scale bars represent 1 µm and 1 second, respectively. Relative Khc-mKate2 (**c**), mCherry-Tm1-I/C (**d**) and GFP-Staufen (**e**) coverage of motile (white) and non-motile (grey) *oskMS2*-GFP trajectories. Numbers within the boxes indicate number of trajectories (number of ooplasms), percentages above the plots show the fraction of RNPs that were found stably and reliably associating with the indicated protein (for at least half of the duration of the trajectory, p<0.01, binominal distribution, see also Supplementary Fig. 3c). P values of pairwise Mann-Whitney U tests are indicated above the boxplots. (**f**) Frequency of Khc-mKate2 appearance on motile (white), before (motility-primed, checked) and after (dotted) the onset of motility, and non-motile (grey) *oskMS2*-GFP trajectories (see also Supplementary Fig. 3d). Fractions within the bars indicate number of association events that lasted longer than a single frame over the number of frames analysed. Indicated P values show results of pairwise Fisher's exact test. The Khc association frequency observed on motility-primed and moving

RNPs is not significantly different from wild-type motile RNP controls (p>0.01). See also Supplementary Fig. 3.

This analysis revealed that in *Khc*^{mKate2} homozygous ooplasmic extracts, close to 50% of motile *oskar* mRNPs are associated with Khc during at least half of the recorded trajectories (Fig. 3c), close to the proportion of plus-end directed runs (65%) (Fig. 1d). In contrast, only ~15% of non-motile mRNPs are associated with Khc during their trajectories. Given that at any given moment most *oskar* particles are stationary (Supplementary Movie 1, Supplementary Table 1)[11, 18, 24], this indicates that the majority of *oskar* mRNPs are not in complex with Khc, which might explain their non-motile status. When we examined Khc association with RNPs in *Tm1*^{gs} mutant extracts, we discovered it was equally low in the motile and non-motile mRNP populations, and that it was considerably below that observed in the wild-type control (Fig. 3c), confirming that Tm1 is required for efficient loading of Khc on *oskar* mRNPs. Our assessment of mCherry-Tm1-I/C association with *oskar* mRNPs revealed a stable association of Tm1-I/C with approximately 20% of mRNPs (Fig. 3b,d), irrespective of the motile/non-motile status of the RNPs (Fig. 3d), similarly to GFP-Staufen (Fig. 3e) and in contrast with Khc-mKate2.

During stage 9 of oogenesis, half of all *oskar* mRNA molecules in the oocyte translocate to the posterior pole[24]. Since only 15% of *oskar* RNPs are in complex with Khc at any given moment (Fig. 3c), this implies that kinesin-1 must dynamically redistribute within the RNP population. By analysing Khc association prior to the onset of *oskar* RNP motility, we detected a slight increase in Khc occupancy on *oskar* mRNPs roughly 4-5 seconds before the start of runs (Supplementary Fig. 3d). Next, we analysed the frequency of the kinesin-1 and *oskar* association events. We observed that motile or motility-primed RNPs are associated with a Khc signal about every 5 seconds (~0.2 s^{-1}, Figure 2F) in wild-type ooplasm. This frequency decreased to ~0.1 s^{-1} in the case of wild-type, non-motile RNPs and dropped to ~0.05 s^{-1} when Tm1-I/C was absent (Fig. 3f). This observation and the low frequency of Khc association we observe in *Tm1*^{gs} mutant ooplasm (Figs. 2d and 3d) provide a mechanistic explanation for the

greatly reduced number of long, unidirectional runs of *oskar* mRNPs in the absence of Tm1-I/C (Supplementary Table 1)[11].

Kinesin-1 is recruited to *oskar* upon nuclear export

To test whether Tm1-I/C and Khc coexist in *oskar* mRNP complexes, we performed *oskar in situ* hybridization on EmGFP-Tm1-I-rescued $Tm1^{gs1}$ mutant egg-chambers carrying one copy of the Khc^{mKate2} allele (Fig. 4a-c'). We found that only small portions of *oskar* mRNPs co-localized with either Khc-mKate2 (~4.6%) or EmGFP-Tm1-I (~5.7%) in the oocytes *in situ* (Fig. 4d), similar to what we observed in our *ex vivo* co-localization analysis (Fig. 2c). Interestingly, the portion of *oskar* mRNPs positive for both Khc-mKate2 and EmGFP-Tm1-I (~5.1%) was statistically not different from the fraction of *oskar* RNPs co-localizing with either of the components. However, it was almost 40% higher than that could be expected based on the observed data ($p=10^{-4}$, Fig. 4d). This suggests that although Khc coverage of *oskar* mRNPs is low, the presence of Tm1-I/C and Khc in the *oskar* transport particles positively correlates.

In the same analysis, we found that the (co-)recruitment of Khc-mKate2 and EmGFP-Tm1-I to *oskar* mRNPs is not restricted to the oocyte, but can be already observed in the nurse cell cytoplasm (Fig. 4a-b',d). By performing STED superresolution microscopy on fixed egg chambers expressing either Khc-EGFP or EmGFP-Tm1-I (Fig. 4e), we confirmed the recruitment of these two components to *oskar* mRNPs in the nurse cells (Fig. 4f,g). Moreover, as observed in the ooplasm, Khc association with *oskar* mRNA was significantly reduced in $Tm1^{gs}$ mutant nurse cells (Fig. 4g).

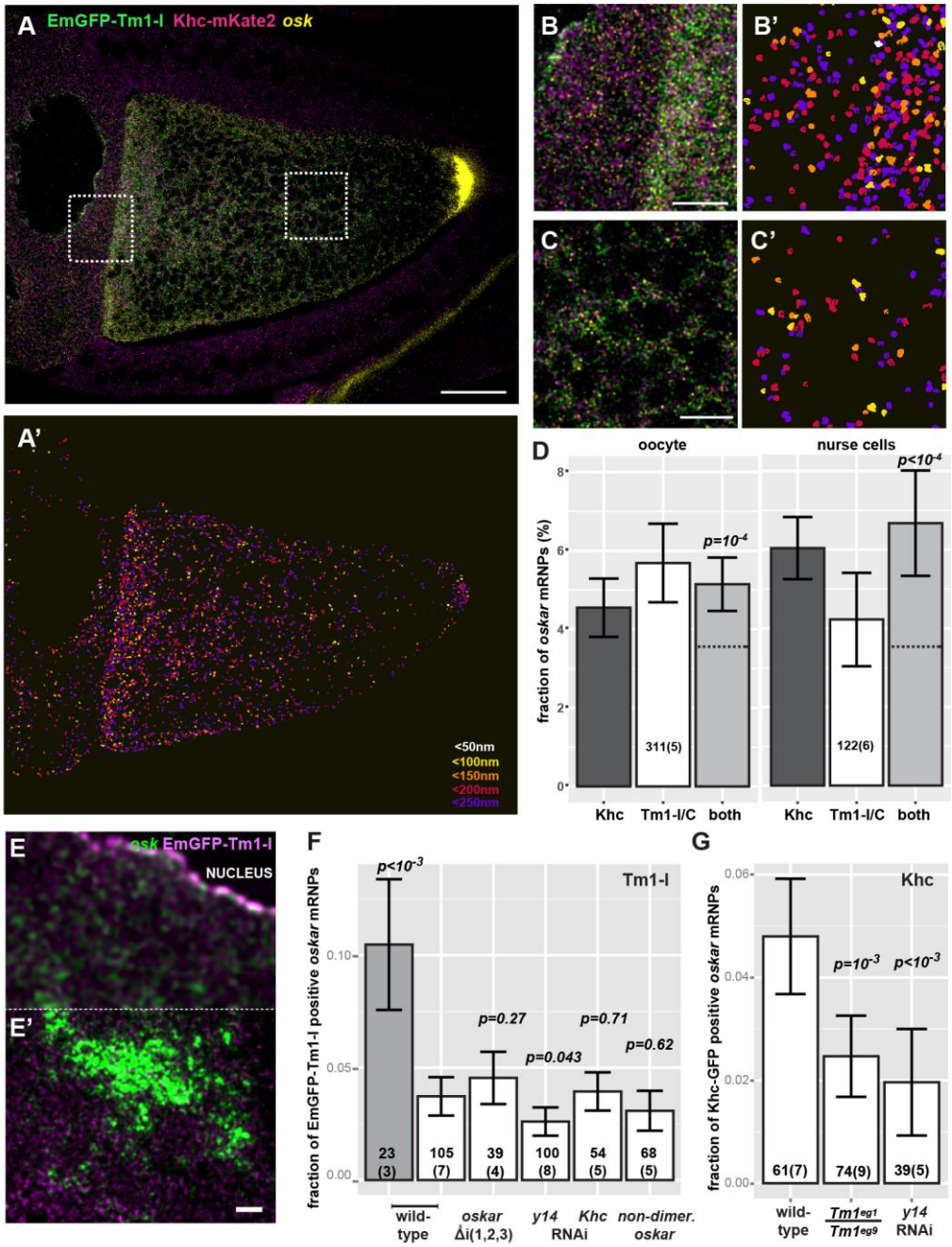

Figure 4: (**a, b, c**) Confocal image of a *Tm1*^{eg9} homozygous egg-chamber expressing EmGFP-Tm1-I (green) and Khc-mKate2 (magenta). *oskar* mRNA labelled with **osk1-5** FIT probes[42] is in yellow. (**a', b', c'**) *oskar* mRNPs co-localizing with both EmGFP-Tm1-I and Khc-mKate2. Colours indicate the maximal co-localization distance (**a'**). Panels **b-c'** represent the boxed regions in panel **a**. (**d**) Fraction of *oskar* mRNPs co-localizing with Khc-mKate (dark grey), EmGFP-Tm1-I (white), or both of these proteins (light grey) in the oocyte or in the nurse cells (max. colocalization distance is 250 nm). None of the values are significantly different from each other (one-way ANOVA, p>10^{-3}). Horizontal dashed lines indicate the expected value of observing both protein in an *oskar* mRNP if the interactions are independent (see Supplementary Fig. 5a,b). P values of one sample t-tests of the observed co-localization values versus these expected values are shown. Confocal (**e**) and gated STED image (**e'**) of EmGFP-Tm1-I expressing nurse cells. GFP auto-fluorescence is in magenta, *oskar* mRNA is in green. (**f**) Fraction of EmGFP-Tm1-I positive *oskar* RNPs (max. colocalization distance is 100 nm) in the indicated nurse cells in the presence of two (gray bar) or one copy (white bars) of the EmGFP-Tm1-I transgene. (**g**) Fraction of Khc-EGFP positive *oskar* RNPs (max. colocalization distance is 100 nm) in the indicated nurse cells. P values of two sample t-tests against wild-type are indicated. Numbers indicate the number of particle

clusters (number of egg-chambers) analysed. Error bars represent 95% confidence intervals. All values (**d, f, g**) are significantly different from zero ($p<10^{-3}$, one sample t-test). Scale bars represent 20 µm (**a**) 5 µm (**b, c**) and 1 µm (**e'**). See also Supplementary Figs. 2 and 4.

EmGFP-Tm1-I –similarly to Khc-mKate2 – localized diffusely in the cytoplasm and, unlike other tropomyosins, did not accumulate on actin structures in the egg-chamber (Supplementary Fig. S4c-d'). In contrast, EmGFP-Tm1-I accumulated at the posterior pole of the oocyte [25] (Supplementary Fig. S4a) and, in the nurse cells, was enriched around the nuclear envelope (NE) (Fig. 5a, Supplementary Fig. S4a); furthermore, the GFP signal was also detected in the nurse cell nuclei (Supplementary Fig. S4b). Remarkably, we found that, in the absence of *oskar* mRNA, EmGFP-Tm1 did not accumulate on the cytoplasmic surface of the NE and was more concentrated in the nuclei than in the cytoplasm (Figs. 5e and 6a,b and Supplementary Fig. 7d,j). These findings suggested that, in the female germline, Tm1-I/C is a nucleocytoplasmic shuttling protein and that its major partner, required for its export, is *oskar* mRNA.

We next examined the distributions of *oskar* mRNA and Khc in the nurse cells. We observed that, like Tm1-I/C, both *oskar* mRNA (Fig. 5b and as reported previously[26]) and Khc enriched around the nurse cell NE (Fig. 5c). By analysing radial profiles of NEs counterstained by fluorescent lectins (Fig. 5a-c), we detected a small but significant perinuclear accumulation of Khc in wild-type nurse cells (Fig. 5d,f), independent of the developmental age of the egg-chamber (Supplementary Fig. 6a). This observed Khc accumulation required the presence of both *oskar* mRNA and of Tm1-I/C (Fig. 5d,f), although *oskar* mRNA accumulation around the NE was not affected in the $Tm1^{gs1}$ egg-chambers (Supplementary Fig. 6b).

Taken together, our results indicate that Khc recruitment to *oskar* takes place as early as upon nuclear export of the mRNPs, around the NE, prior to the actual involvement of kinesin-1 in the *oskar* localization process. Furthermore, the recruitment of the kinesin-1 motor requires the presence of Tm1-I/C on *oskar* mRNPs.

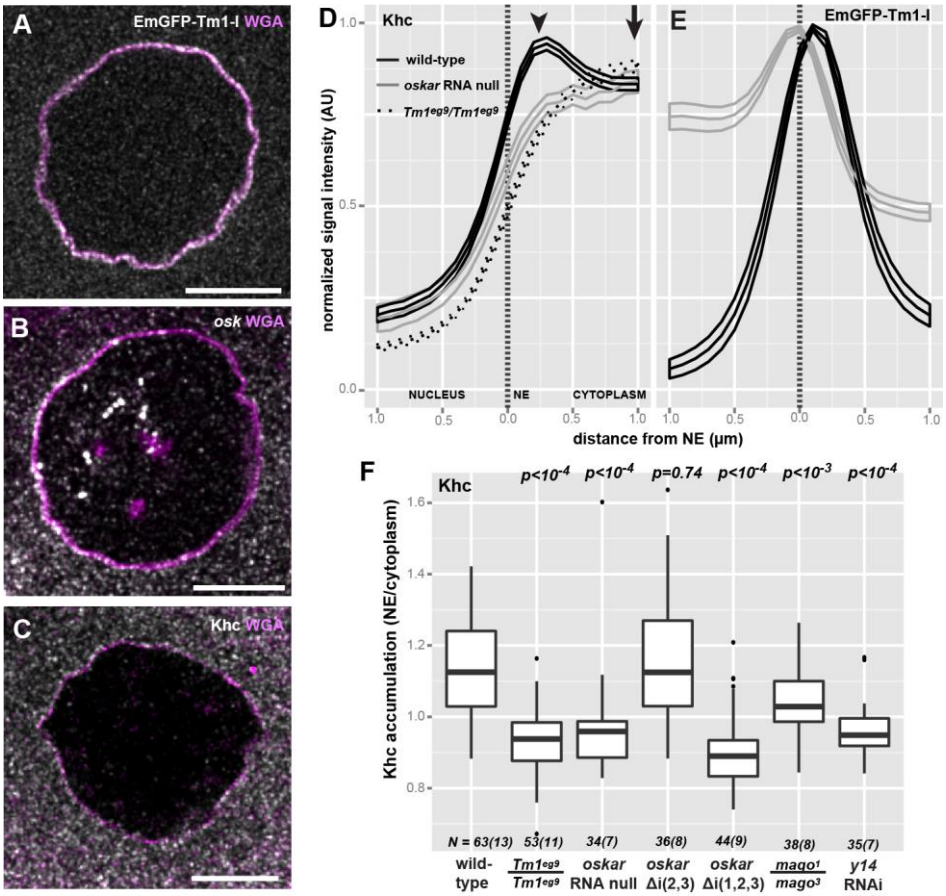

Figure 5: Localization of EmGFP-Tm1-I (**a**) *oskar* mRNA (**b**) and Khc (**c**) around the nurse cell nuclear envelope (magenta, WGA staining). Mean distribution profile of Khc (**d**) and EmGFP-Tm1-I (**e**) around the NE of nurse cells (marked with a dotted vertical line). Genotypes are indicated as follows: wild-type control with solid black line, *oskar* RNA null with solid gray line, $Tm1^{eg9}/Tm1^{eg9}$ with dotted black line (mean±95% conf. int.). (**f**) Khc accumulation around the NE. To calculate accumulation the signal intensity measured at the position of wild-type peak (arrowhead, 356±17.6 nm away from NE) divided by signal intensity 2 SD away (arrow, at 356+2*410 nm). P values of pairwise Mann-Whitney U tests against wild-type control are indicated above the boxplots. Numbers indicate the number of nuclei (number of egg-chambers) analysed. See also Supplementary Fig. 6.

oskar 3'UTR recruits Tm1-I/C

To determine what element(s) in *oskar* mRNA are responsible for Tm1-I/C and eventually Khc recruitment, we systematically replaced wild-type *oskar* mRNA with different truncations and mutant versions of the mRNA, expressed from transgenes in the egg-chamber. A compromised EJC or SOLE causes *oskar* mRNA motility and localization defects similar to those observed in $Tm1^{gs}$ mutants[11, 18]. We therefore tested whether the association of Khc with *oskar* RNPs is affected when the EJC/SOLE functional unit fails to form. Either disruption of the EJC or substitution of wild-type *oskar* mRNA with the non-spliced *oskar Δi(1,2,3)* resulted

in a loss of Khc accumulation around the NE (Fig. 5f and Supplementary Fig. 6c). Also, the fraction of Khc-positive *oskar* mRNPs was significantly reduced upon knocking down levels of the EJC core component Y14 (Fig. 4g).

Interestingly, we observed no significant effect on NE localization and nuclear accumulation of EmGFP-Tm1-I in *oskar Δi(1,2,3)* expressing oocytes (Fig 6a,b and Supplementary Fig. 6f,j) and EmGFP-Tm1-I association with *oskar* mRNPs was also unaffected (Fig. 4f). In contrast, expression of a spliced *oskar* version lacking the *oskar* 3' UTR (*osk-bcd*)[12], resulted in an aberrant Tm1-I/C distribution, similar to what was observed in absence of *oskar* mRNA (Fig 6a,b and Supplementary Fig. 6g,j). The smallest unit capable of restoring a wild-type Tm1-I/C localization was the intact *oskar* 3'UTR (Fig 6a,b and Supplementary Fig. 6e,j). Truncations of the 3'UTR[10] and a mere two nucleotide substitution in the kissing loop that mediates *oskar* mRNA dimerization[27] greatly reduced EmGP-Tm1-I accumulation near the cytoplasmic surface of the NE and led to concentration of Tm1-I/C in the nuclei (Fig 6a,b and Supplementary Fig. 6h-j). As the fraction of non-dimerizing *oskar* mRNPs associated with EmGFP-Tm1-I did not differ from the wild-type control (Fig. 4f), we hypothesize that a higher nuclear EmGFP-Tm1-I concentration compensates for its lower affinity for this *oskar* species. Nevertheless, the non-dimerizing *oskar* mRNA - whose localization appeared qualitatively normal (Supplementary Fig. 8a)[27] – showed a reduced efficiency of posterior-ward translocation (Fig. 7k,l).

These results indicate that Tm1-I/C recruits Khc independently of the EJC/SOLE – which also contributes to Khc recruitment- and requires an intact, dimerization-competent *oskar* 3' UTR for its association with *oskar* mRNPs.

Tm1-I binds directly to the *oskar* 3' UTR

In a screen to identify proteins bound directly to mRNAs in early *Drosophila* embryos, we isolated an isoform-non-specific Tm1 peptide[28]. By immunoprecipitating EmGFP-Tm1-I from lysates of embryos exposed to 254nm UV light, we detected significantly more poly(A)+ RNAs

cross-linked to Tm1-I/C than to the control (Supplementary Fig. 7a,a'), confirming the RNA binding activity of TM1-I/C. qRT-PCR of cross-linked mRNAs revealed *oskar* as a target of TM1-I/C (Supplementary Fig. 7b). To identify the region of *oskar* mRNA to which Tm1-I/C binds, we incubated the embryonic lysates expressing EmGFP-Tm1-I with exogenous digoxygenin-labelled *oskar* RNA fragments and subjected them to UV cross-linking. Immunoprecipitation allowed the recovery of the *oskar* 3'UTR, but not of other regions of the mRNA (Fig. 6c,d). Truncated (Supplementary Fig. 7k,l) and the non-dimerizing *oskar* 3'UTR (Fig. 6e) bound to EmGFP-Tm1-I with reduced affinity. These findings also suggest that efficient direct binding of Tm1-I/C to *oskar* mRNPs requires an intact, dimerizing *oskar* 3'UTR.

It has been reported that *oskar* mRNA dimers and higher order assemblies are promoted or stabilized by RNA binding proteins, such as Bruno[29] and Polypyrimidine tract binding protein (PTB)[30]. To test if Tm1-I/C possesses similar activity, we targeted *oskar* mRNA with two orthogonally labelled probes of identical sequence specificity (Fig. 6f). This analysis revealed a substantial reduction in the fraction of *oskar* mRNPs containing multiple copies of the mRNA in *Tm1*^{gs} mutant nurse cells, as we also observed in the absence of PTB (Fig. 6g and Supplementary Fig. 7m), indicating the interdependence of *oskar* mRNA dimerization and Tm1-I/C recruitment.

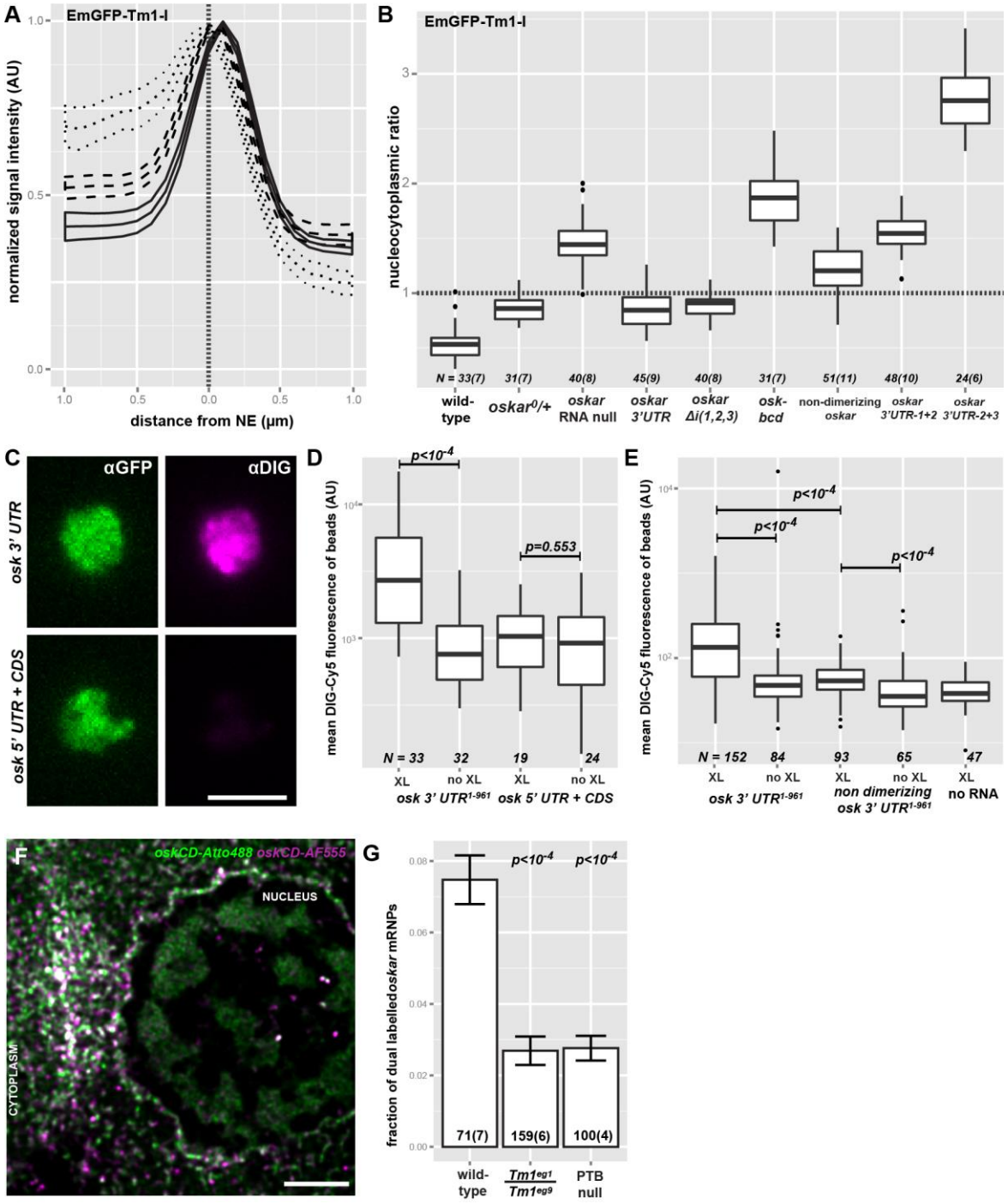

Figure 6: (**a**) Distribution of EmGFP-Tm1-I around the nurse cell NE in egg-chambers. *osk-bcd* is indicated with dotted, non-dimerizing *oskar* with dashed and *oskar* 3' UTR with solid line (mean±95% conf. int.). (**b**) Nucleocytoplasmic distribution of EmGFP-Tm1-I. Ratios of the mean signal intensity measured at a distance of one to two microns from the NE, within and outside of the nucleus were calculated. All values are significantly different from one ($p<10^{-3}$, one sample t-test). Numbers indicate the number of nurse cell nuclei (number of egg-chambers) analysed. (**c**) Images of beads binding to EmGFP-Tm1-I (green) and DIG labelled *in vitro* transcribed RNA fragments (magenta). (**d, e**) Mean DIG-Cy5 fluorescence measured on beads capturing the RNA fragment, with or without UV cross-linking, indicated below the charts. P values of pairwise Mann-Whitney U tests are indicated. In panel **e**, none of the non-cross-linked samples differ significantly from the no RNA control ($p>0.05$). (**f**) Competitive FISH of *oskar* mRNA in a wild-type nurse cell. (**g**) Fraction of *oskar* mRNPs labelled non-randomly with both colours during competitive FISH in nurse cells of the indicated genotypes (both

colours found within 100 nm, mean±95% conf. int.). P values of two sample t-tests against wild-type are indicated. Numbers indicate the number of particle clusters (number of egg-chambers) analysed. Scale bars represent 5 µm. See also Supplementary Figs. 7 and 8.

Partially interchangeable roles of Tm1-I/C and the EJC/SOLE

We noted that transgenic over-expression of EmGFP-Tm1-I increased Khc recruitment to the NE substantially in the rescued *Tm1*^{gs} egg-chambers (Fig. 7a,e). Although there was a slight yet significant elevation in Khc accumulation in the absence of *oskar* RNA, which might reflect the presence of other, even non-specific mRNA targets of over-expressed EmGFP-Tm1-I, substantial increase was only observed when the intact *oskar* 3'UTR was present (Fig. 5b-e). To address the functional consequences of this 'super-loading' of Khc, we quantified the mean distribution of *oskar Δi(1,2,3)* RNA throughout stage 9 oocytes[24]. This analysis showed that over-expression of EmGFP-Tm1-I causes a posterior-ward shift of the otherwise non-localizing mRNA (Fig. 7f,g,l). However, this rescue was not complete as it still significantly deviated from the wild-type control. Furthermore, EmGFP-Tm1-I over-expression did not promote posterior localization of the RNA consisting solely of the *oskar* 3'UTR (Fig. 7i,l), despite the increased recruitment of Khc to the NE. EmGFP-Tm1-I over-expression also did not promote *oskar* mRNA localization in oocytes with reduced Khc levels (Fig. 7j,l), confirming the essential role of kinesin-1 motor is this process. These observations indicate that a properly assembled EJC/SOLE is required to activate the *oskar* bound, Tm1-I/C recruited kinesin-1 within the oocyte.

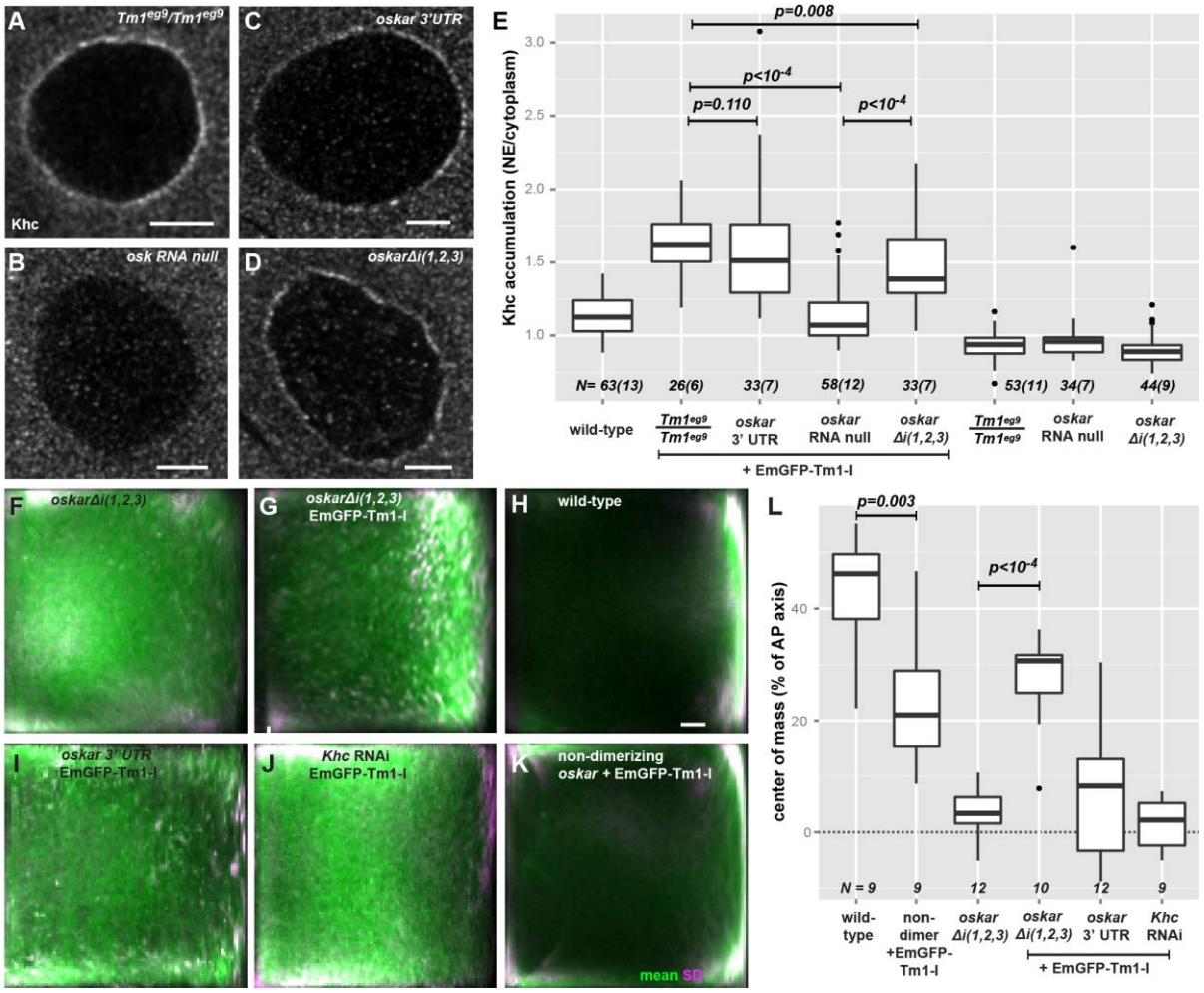

Figure 7: (**a-d**) Khc accumulation around the NE of nurse cells over-expressing EmGFP-Tm1-I within *Tm1*^{eg9}*/Tm1*^{eg9} (**a**), and *oskar* RNA null egg-chambers (**b**) expressing either the *oskar* 3' UTR (**c**) or *oskar Δi(1,2,3)* (**d**). Scale bars are 5 µm. (**e**) Khc accumulation around the nurse cell NE. P values of pairwise Mann-Whitney U tests are indicated. Numbers indicate the number of nurse cell nuclei (number of egg-chambers) analysed. (f-k) Mean *oskar* mRNA distribution (green) within oocytes in which *oskar* mRNA is substituted by *oskar Δi(1,2,3)* mRNA (**f**, **g**), *oskar* 3'UTR mRNA (**i**) or non-dimerizing *oskar* mRNA (**k**) and that (in addition) over-express EmGFP-Tm1-I (**g**, **i** and **k**). Wild-type control (**h**) and oocytes expressing *Khc* RNAi and EmGFP-Tm1-I (**j**). (**h**) Scale bar is 10% of total oocyte length. (**l**) Position of the *oskar* mRNA center of mass relative to the geometric center of the oocyte (dotted horizontal line) along the anteroposterior (AP) axis. Posterior pole is the top of the chart. P values of pairwise Mann-Whitney U tests are indicated. Numbers indicate number of oocytes analysed. See also Supplementary Fig. 8.

Discussion

Our findings show that Khc is recruited to *oskar* mRNA in the perinuclear cytoplasm of the nurse cells through the concerted actions of Tm1-I/C and the EJC/SOLE complex, both of which associate with *oskar* mRNA in the nucleus (Fig. 8). This early recruitment of Khc to

oskar RNPs was unexpected, as the first step of *oskar* transport, from the nurse cells into the oocyte, is mediated by by cytoplasmic dynein[9, 10]. Dynein is presumably also recruited at the NE, where we also detected accumulation of the cargo adapter Egalitarian[5, 31] and the dynactin component Dynamitin[32]. Interestingly, the dynein apoenzyme did not enrich around the NE (Supplementary Fig. 8b-e), possibly because its association with *oskar* mRNPs instantly initiates their transport into the oocyte. The presence of the two opposite polarity motors on *oskar* mRNPs calls for regulators that coordinate motor action responding either to environmental changes[24, 33] or to the developmental program: the failed or incomplete posterior localization of *oskar* 3'UTR and *oskar Δi(1,2,3)*, respectively, indicates that the presence of Khc on the RNPs is necessary but not sufficient for proper *oskar* localization. Since the *oskar* coding sequence – with the exception of the SOLE – was shown to be dispensable for the localization process[18], we propose that the *oskar* mRNA targeting to the posterior pole depends on two independent elements: 1) the spliced, EJC associated SOLE complex, which activates *oskar* bound kinesin-1 in the oocyte in a context-sensitive manner and 2) the *oskar* 3' UTR, which recruits cytoplasmic dynein[10] and kinesin-1, the latter through Tm1-I/C. Our data suggest that Khc recruitment may depend on dimerization of *oskar* mRNA, as this process facilitates Tm1-I/C binding. Consistent with this, cytoplasmic *oskar* transport particles have been shown to contain at least two *oskar* mRNA molecules[26] and defects of oligomarization result in improper localization of *oskar*[30, 34]. Since we detected no interaction between the EJC/SOLE and Tm1-I/C/3'UTR kinesin-1 recruitment and activation appears to be modular.

Our work shows that Khc recruitment is dynamic and that this dynamicity depends on Tm1-I/C. Although the mechanism behind it is cryptic, the dynamic loading and unloading of kinesin-1 provides an economical and efficient means to localize the estimated ~1.25-7.5x10^5 *oskar* transport particles (I.G., unpublished data) within a few hours[24], when at any given moment only a small subset of *oskar* mRNPs is available and in complex with Khc. We think that the modularity, the dynamicity and the complex, coordinated motor activity makes *oskar* mRNPs

model cargoes for discovering novel modes of mechanoenzyme regulation and deciphering the logic of organelle distribution.

The finding that Khc does not accumulate around nurse cell NEs in the absence of *oskar* mRNA suggests that it is the main, if not the sole mRNA in the *Drosophila* germline to be transported actively by kinesin-1 to the posterior pole of the oocyte. Consistent with this, a recent study of mRNA localization in the developing egg-chamber showed that all posterior targeted mRNAs analysed require localized *oskar* mRNA and/or locally translated Oskar protein for their localization[35]. However, Tm1-I/C appears to have other target mRNAs within the organism, as *coracle* mRNA localization to neuromuscular junctions is affected in $Tm1^{gs}$ mutants[36]. Future identification of these target mRNAs should reveal the RNA features that prime mRNPs for transport by kinesin-1.

Tm1-I/C is an unusual tropomyosin: although it has a short tropomyosin superfamily domain in its C-terminal moiety, its N-terminal portion consists almost entirely of low complexity sequence[25] and the protein forms intermediate filament like structures *in vitro*[25]. Proteins containing disordered regions are major constituents of RNA containing membraneless organelles, such as RNA granules[37], stress granules[38], P granules[39], nuage and germ granules[40]. Although orthologues of the Tm1-I/C N-terminal region are not present beyond *Diptera*, the juxtaposition of low complexity sequences with cytoskeleton binding domains as a module allowing recruitment of motor proteins to mRNAs may be conserved among higher eukaryotes including mammals. For instance, the non-homologous actin-binding proline-rich murine synaptopodin protein was shown to rescue mislocalization of *oskar* mRNA in $Tm1^{gs}$ mutant oocytes although the basis of this rescue was not addressed[41]. Further dissection of the precise molecular functions of Tm1-I/C – and of synaptopodin - in *oskar* mRNP assembly will be crucial to determining the nature and the minimal number of features necessary for kinesin-1 mediated localization of mRNPs in eukaryotes.

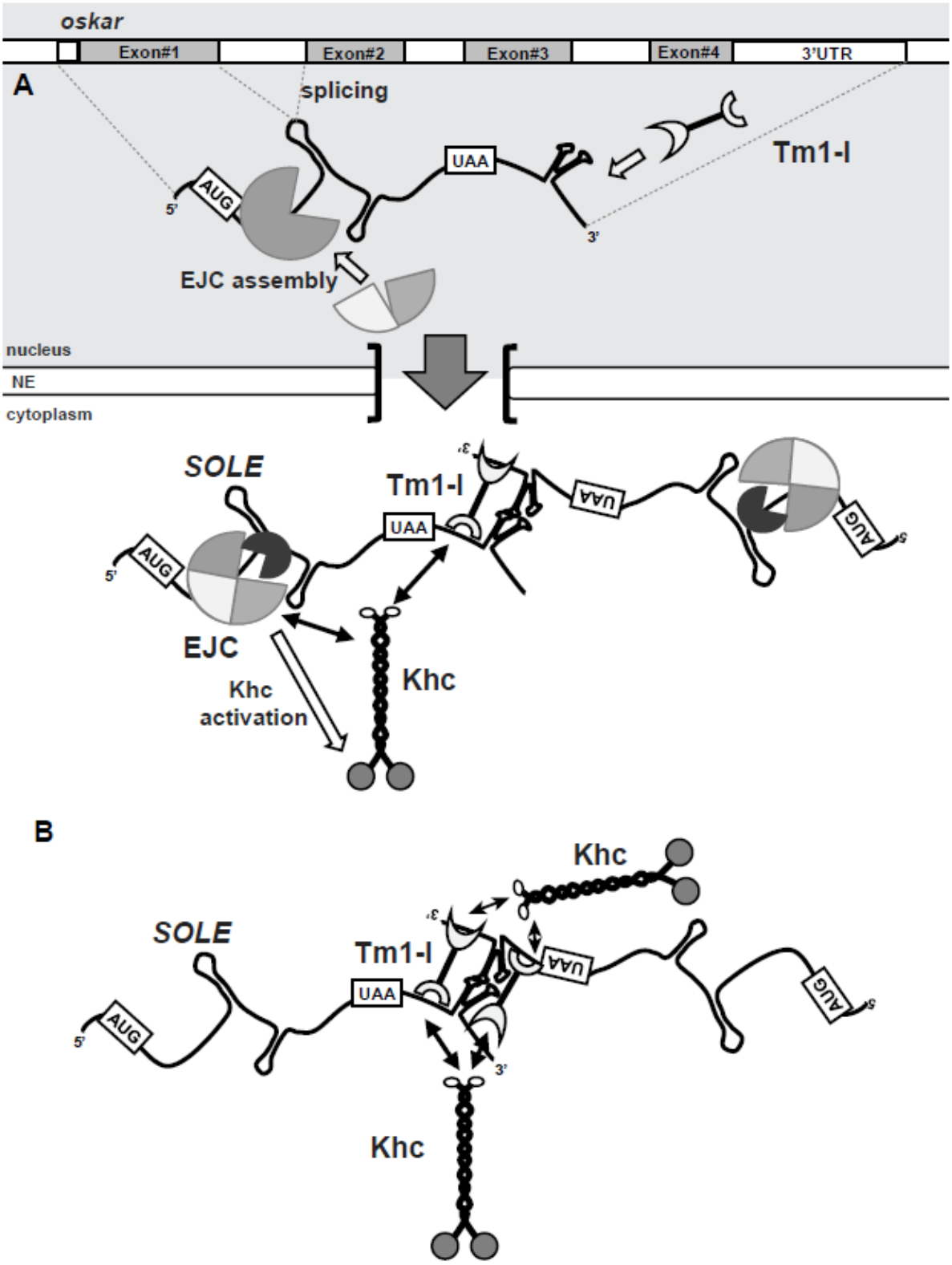

Figure 8: Proposed mechanism of Khc recruitment by Tm1-I/C and SOLE-associated EJC to *oskar* mRNA dimers upon their export from nurse cell nuclei. (**a**) In wild-type nurse cells, the core components of the EJC and Tm1-I/C are recruited to *oskar* mRNA within the nucleus, upstream of the SOLE and to the 3' UTR, respectively. Upon nuclear export, EJC and Tm1-I/C coordinate the recruitment of kinesin-1 (Khc). The EJC in conjunction with the SOLE is required for kinesin-1 activation, while Tm1-I/C is required to maintain dynamic loading of the motor in the oocyte. (**b**) Overexpression of EmGFP-Tm1-I results in the overloading of kinesin-1 on *oskar* mRNPs, even when EJC/SOLE assembly is

compromised. This kinesin-1 overloading is possibly due to saturation of symmetric Tm1-I/C binding sites in the dimerizing *oskar* 3' UTRs upon EmGFP-Tm1-I overexpression.

Author contributions

IG and AE conceived the experiments and wrote the manuscript. VS carried out qRT-PCR analysis of mRNAs immunoprecipitated under stringent conditions. AK synthesized the *oskar* probes and carried out the competitive FISH experiments. The rest of the experiments and data analysis were carried out by IG.

Acknowledgements

We thank Denise Montell for sharing unpublished data, antibodies and discussions. We thank Damian Brunner, Tze-Bin Chou, Elizabeth Gavis, Antoine Guichet, Daniel St Johnston and the Developmental Studies Hybridoma Bank for fly stocks and reagents, and the TRiP at Harvard Medical School (NIH/NIGMS R01-GM084947) for transgenic RNAi fly stocks used in this study. Stocks obtained from the Bloomington *Drosophila* Stock Center (NIH P40OD018537) were used in this study. We are grateful to Frank Wippich for his comments on the manuscript. We thank Sandra Müller and Alessandra Reversi for fly transgenesis, the EMBL Advanced Light Microscopy Facility and Leica for providing cutting-edge microscopy, and the EMBL Genomics Core Facility for their help with qRT-PCR. This work was funded by the EMBL.

References

1. Hirokawa, N., Niwa, S. & Tanaka, Y. Molecular motors in neurons: transport mechanisms and roles in brain function, development, and disease. *Neuron* **68**, 610-638 (2010).
2. Medioni, C., Mowry, K. & Besse, F. Principles and roles of mRNA localization in animal development. *Development* **139**, 3263-3276 (2012).
3. Marchand, V., Gaspar, I. & Ephrussi, A. An intracellular transmission control protocol: assembly and transport of ribonucleoprotein complexes. *Curr Opin Cell Biol* **24**, 202-210 (2012).
4. Bullock, S.L., Ringel, I., Ish-Horowicz, D. & Lukavsky, P.J. A'-form RNA helices are required for cytoplasmic mRNA transport in Drosophila. *Nat Struct Mol Biol* **17**, 703-709 (2010).
5. Dienstbier, M., Boehl, F., Li, X. & Bullock, S.L. Egalitarian is a selective RNA-binding protein linking mRNA localization signals to the dynein motor. *Genes Dev* **23**, 1546-1558 (2009).
6. Dix, C.I. *et al.* Lissencephaly-1 promotes the recruitment of dynein and dynactin to transported mRNAs. *J Cell Biol* **202**, 479-494 (2013).
7. Niedner, A., Edelmann, F.T. & Niessing, D. Of social molecules: The interactive assembly of ASH1 mRNA-transport complexes in yeast. *RNA Biol* **11**, 998-1009 (2014).
8. Gagnon, J.A., Kreiling, J.A., Powrie, E.A., Wood, T.R. & Mowry, K.L. Directional transport is mediated by a Dynein-dependent step in an RNA localization pathway. *PLoS Biol* **11**, e1001551 (2013).
9. Clark, A., Meignin, C. & Davis, I. A Dynein-dependent shortcut rapidly delivers axis determination transcripts into the Drosophila oocyte. *Development* **134**, 1955-1965 (2007).
10. Jambor, H., Mueller, S., Bullock, S.L. & Ephrussi, A. A stem-loop structure directs oskar mRNA to microtubule minus ends. *RNA* **20**, 429-439 (2014).
11. Zimyanin, V.L. *et al.* In vivo imaging of oskar mRNA transport reveals the mechanism of posterior localization. *Cell* **134**, 843-853 (2008).
12. Ephrussi, A. & Lehmann, R. Induction of germ cell formation by oskar. *Nature* **358**, 387-392 (1992).
13. Ephrussi, A., Dickinson, L.K. & Lehmann, R. Oskar organizes the germ plasm and directs localization of the posterior determinant nanos. *Cell* **66**, 37-50 (1991).
14. Kim-Ha, J., Smith, J.L. & Macdonald, P.M. oskar mRNA is localized to the posterior pole of the Drosophila oocyte. *Cell* **66**, 23-35 (1991).
15. Loiseau, P., Davies, T., Williams, L.S., Mishima, M. & Palacios, I.M. Drosophila PAT1 is required for Kinesin-1 to transport cargo and to maximize its motility. *Development* **137**, 2763-2772 (2010).
16. Brendza, R.P., Serbus, L.R., Duffy, J.B. & Saxton, W.M. A function for kinesin I in the posterior transport of oskar mRNA and Staufen protein. *Science (New York, N.Y* **289**, 2120-2122 (2000).
17. Hachet, O. & Ephrussi, A. Splicing of oskar RNA in the nucleus is coupled to its cytoplasmic localization. *Nature* **428**, 959-963 (2004).
18. Ghosh, S., Marchand, V., Gaspar, I. & Ephrussi, A. Control of RNP motility and localization by a splicing-dependent structure in oskar mRNA. *Nat Struct Mol Biol* **19**, 441-449 (2012).
19. Erdelyi, M., Michon, A.M., Guichet, A., Glotzer, J.B. & Ephrussi, A. Requirement for Drosophila cytoplasmic tropomyosin in oskar mRNA localization. *Nature* **377**, 524-527 (1995).
20. Sanghavi, P., Laxani, S., Li, X., Bullock, S.L. & Gonsalvez, G.B. Dynein associates with oskar mRNPs and is required for their efficient net plus-end localization in Drosophila oocytes. *PLoS One* **8**, e80605 (2013).
21. Soundararajan, H.C. & Bullock, S.L. The influence of dynein processivity control, MAPs, and microtubule ends on directional movement of a localising mRNA. *Elife* **3**, e01596 (2014).
22. Telley, I.A., Bieling, P. & Surrey, T. Obstacles on the microtubule reduce the processivity of Kinesin-1 in a minimal in vitro system and in cell extract. *Biophys J* **96**, 3341-3353 (2009).

23. Sung, H.H. *et al.* Drosophila ensconsin promotes productive recruitment of Kinesin-1 to microtubules. *Dev Cell* **15**, 866-876 (2008).
24. Gaspar, I. *et al.* Klar ensures thermal robustness of oskar localization by restraining RNP motility. *J Cell Biol* **206**, 199-215 (2014).
25. Cho, A., Kato, M., Whitwam, T., Kim, J.H. & Montell, D.J. An Atypical Tropomyosin in Drosophila with Intermediate Filament-like Properties. *Cell Rep* **16**, 928-938 (2016).
26. Little, S.C., Sinsimer, K.S., Lee, J.J., Wieschaus, E.F. & Gavis, E.R. Independent and coordinate trafficking of single Drosophila germ plasm mRNAs. *Nat Cell Biol* **17**, 558-568 (2015).
27. Jambor, H., Brunel, C. & Ephrussi, A. Dimerization of oskar 3' UTRs promotes hitchhiking for RNA localization in the Drosophila oocyte. *RNA* **17**, 2049-2057 (2011).
28. Sysoev, V.O. *et al.* Global changes of the RNA-bound proteome during the maternal-to-zygotic transition in Drosophila. *Nat Commun* **7**, 12128 (2016).
29. Chekulaeva, M., Hentze, M.W. & Ephrussi, A. Bruno acts as a dual repressor of oskar translation, promoting mRNA oligomerization and formation of silencing particles. *Cell* **124**, 521-533 (2006).
30. Besse, F., Lopez de Quinto, S., Marchand, V., Trucco, A. & Ephrussi, A. Drosophila PTB promotes formation of high-order RNP particles and represses oskar translation. *Genes Dev* **23**, 195-207 (2009).
31. Navarro, C., Puthalakath, H., Adams, J.M., Strasser, A. & Lehmann, R. Egalitarian binds dynein light chain to establish oocyte polarity and maintain oocyte fate. *Nat Cell Biol* **6**, 427-435 (2004).
32. McGrail, M. *et al.* Regulation of cytoplasmic dynein function in vivo by the Drosophila Glued complex. *J Cell Biol* **131**, 411-425 (1995).
33. Burn, K.M. *et al.* Somatic insulin signaling regulates a germline starvation response in Drosophila egg chambers. *Dev Biol* **398**, 206-217 (2015).
34. Reveal, B. *et al.* BREs mediate both repression and activation of oskar mRNA translation and act in trans. *Dev Cell* **18**, 496-502 (2010).
35. Jambor, H. *et al.* Systematic imaging reveals features and changing localization of mRNAs in Drosophila development. *Elife* **4** (2015).
36. Gardiol, A. & St Johnston, D. Staufen targets coracle mRNA to Drosophila neuromuscular junctions and regulates GluRIIA synaptic accumulation and bouton number. *Dev Biol* **392**, 153-167 (2014).
37. Kato, M. *et al.* Cell-free formation of RNA granules: low complexity sequence domains form dynamic fibers within hydrogels. *Cell* **149**, 753-767 (2012).
38. Molliex, A. *et al.* Phase Separation by Low Complexity Domains Promotes Stress Granule Assembly and Drives Pathological Fibrillization. *Cell* **163**, 123-133 (2015).
39. Elbaum-Garfinkle, S. *et al.* The disordered P granule protein LAF-1 drives phase separation into droplets with tunable viscosity and dynamics. *Proc Natl Acad Sci U S A* **112**, 7189-7194 (2015).
40. Nott, T.J. *et al.* Phase transition of a disordered nuage protein generates environmentally responsive membraneless organelles. *Mol Cell* **57**, 936-947 (2015).
41. Wong, J.S. *et al.* Rescue of tropomyosin deficiency in Drosophila and human cancer cells by synaptopodin reveals a role of tropomyosin alpha in RhoA stabilization. *EMBO J* **31**, 1028-1040 (2012).
42. Hovelmann, F. *et al.* Brightness through local constraint--LNA-enhanced FIT hybridization probes for in vivo ribonucleotide particle tracking. *Angew Chem Int Ed Engl* **53**, 11370-11375 (2014).